Quantitative Study of Electron Transport in Ballistic-Electron-Emission Microscopy

A. Bauer, M. T. Cuberes,* M. Prietsch, and G. Kaindl
Institut für Experimentalphysik, Freie Universität Berlin, Arnimallee 14, W-1000 Berlin 33, Germany
(Received 30 November 1992)

Ballistic-electron-emission microscopy (BEEM) of Au and Mg films on *n*-type GaP(110), with thicknesses as low as 12 Å, reveals strong variations of spectral shape and magnitude of the BEEM current with metal-film thickness and surface gradient. Using Monte Carlo simulations, the hot-electron transport between tip and semiconductor can be quantitatively described, providing detailed information on tunneling, transport in the metal, transmission across the interface, and impact ionization in the semiconductor.

PACS numbers: 73.40.−c, 72.10.Bg, 73.50.Gr

Ballistic-electron-emission microscopy (BEEM) is by now a well-established technique, based on the scanning tunneling microscope (STM), for the study of semiconductor interfaces with extremely high lateral resolution [1]. In a typical BEEM experiment, electrons tunnel from a negatively biased tip into a metal film grown on an *n*-type semiconductor; if the film is thin enough, some of these electrons will reach the metal-semiconductor interface ballistically, i.e., without scattering. At electron energies exceeding the threshold for injection into the semiconductor, a collector or BEEM current I_B is observed. In this way, BEEM allows a spectroscopic determination of local Schottky-barrier heights. In addition, the homogeneity of the interface can be studied by simultaneously taking topographic and BEEM-current images. Despite this considerable potential inherent in BEEM, the detailed theoretical understanding of electron transport between tip and semiconductor is still rather poor, since only a few approaches have been performed up to now [2–7].

In this Letter, we present the results of a systematic BEEM study of interfaces of Au and Mg with *n*-type GaP(110), with film thicknesses as low as 12 Å, just above the onset of metallicity. In the BEEM spectra recorded for tip voltages V_T up to 6 eV, significant variations in spectral shape and magnitude of the BEEM current with metal-film thickness were found. In addition, BEEM-current images of (12 Å Au)/GaP(110) show a strong influence of surface topography. These observations are well reproduced by the results of Monte Carlo simulations of the hot-electron transport between tip and semiconductor. In this way, tunneling from tip to metal, inelastic and elastic scattering in the metal, transmission across the interface, and impact ionization in the semiconductor were described quantitatively. The simulations reveal that—in the present cases—(i) impact ionization contributes to the BEEM current at $V_T > 4$ eV, (ii) interface transmission is well described using a simple free-electron approximation in both the metal and the semiconductor, and (iii) strong elastic scattering occurs in the metal film with a mean free path of only $\simeq 30$ Å.

Sample preparation and BEEM measurements were performed in ultrahigh vacuum (5×10^{-11} mbar), using an STM that has been described elsewhere [8,9]. *n*-type GaP (doped with $\simeq 2\times10^{18}$ sulfur atoms/cm^3) was cleaved *in situ* and subsequently covered with Au and Mg films. Au was evaporated from a Au wire, coiled around a Mo bushel serving as a filament, while Mg was evaporated from a quartz crucible. During evaporation, the pressure rose to 1×10^{-9} mbar for Au and 1×10^{-10} mbar for Mg. Growth rates were monitored by a quartz microbalance with an accuracy of $\simeq 30\%$. Chemically etched W tips, cleaned *in situ* by electron bombardment, were used for tunneling, and a Au wire for contacting the metal layer. BEEM data were taken at constant tunneling currents I_T around 1 nA. Even at the lowest metal-film thickness (12 Å), the conductance of the metal layer was found to be sufficiently high to avoid tip-induced charging.

Representative BEEM spectra for Au and Mg films on *n*-type GaP(110) are presented in Fig. 1, revealing significant differences in spectral shape and magnitude of the BEEM current for the two metals and the two film thicknesses. The spectrum for 50 Å Mg shows an overshoot at $V_T = 1.8$ eV, while additional thresholds are observed in the other spectra at $V_T \simeq 4$ eV. Furthermore, BEEM currents of up to 40% of the tunnel current were observed in case of 12 Å Au, while they were less than 0.5% for 50 Å Mg. To account for these variations, Monte Carlo simulations for the hot-electron transport from tip to semiconductor were carried out, applying a four-step model [10]: tunneling from tip to metal, transport through the metal film, transmission across the interface, and impact ionization in the semiconductor depletion zone.

The tunneling probability P_T, as a function of electron energy E and emission angle with respect to the surface normal ϑ, can be approximated by

$$P_T \propto \exp\left(\frac{E}{\Delta E_T}\right)\exp\left(-\frac{\vartheta^2}{2\Delta\vartheta_T^2}\right).$$

Here, the energy dependence is derived from planar-

0031-9007/93/71(1)/149(4)$06.00

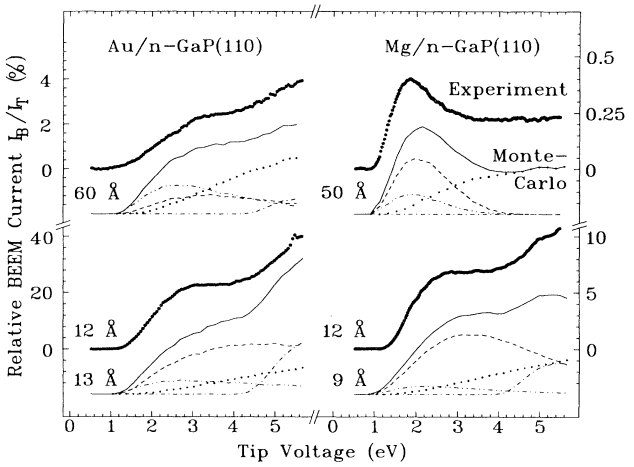

FIG. 1. BEEM spectra (filled circles) and results of Monte Carlo simulations (solid curves) for various film thicknesses of Mg and Au on *n*-type GaP(110). The theoretical curves are decomposed into contributions from ballistic electrons that have suffered no scattering at all (dashed), electrons scattered only elastically (dash-double dotted), inelastically scattered plus secondary electrons (dotted), and additional electrons created by impact ionization (dash-dotted).

tunneling theory [11], where ΔE_T is the width of the energy distribution, amounting to about 0.4 eV in the present case. The weak dependence of ΔE_T on the tip-to-metal spacing ($\simeq 7$ Å), the tunneling barrier, and the tip voltage was taken into account in the present calculations. The angular distribution is characterized by $\Delta\vartheta_T$, which is expected to be in the order of 20° [9,10]. In the presence of a surface gradient, the emission characteristics are tilted with respect to the interface.

In order to describe the electron transport through the metal film, the electrons are treated as quasifree particles suffering inelastic and elastic scattering. In the present context, elastic scattering includes quasielastic phonon scattering, since the energy loss is not significant for BEEM. In the energy range of interest, inelastic scattering is mainly due to electron-electron interactions, and the energy dependence of the mean free path λ_{in} is given by [12]

$$\lambda_{in}=\lambda_{in}^{0}\frac{E/E_F^m}{(E-E_F^m)^2};$$

here, E_F^m represents the Fermi energy in the metal, and E is the electron energy relative to the conduction-band minimum of the metal. Considering the number of possible transitions on the assumption of a constant density of states, the probability for the primary electron to lose an energy ΔE is proportional to ΔE, with the energy of the secondary electron equally distributed between E_F^m and $E_F^m+\Delta E$. In the case of elastic scattering, an energy-independent mean free path λ_{el} is assumed [13]. In both cases, the angular distributions of the outgoing electrons are assumed to be isotropic. At the metal surface, where local height variations are neglected, as well as in the case of total reflection at the interface, elastic backscattering with an isotropic angular distribution is assumed. This is justified since the metal surface is usually rough, and stronger elastic scattering is expected to occur close to the interface because of intense interfacial reactions, which have been observed for Au and Mg on GaP(110) using core-level photoemission [14]. The calculated random walks of all primary and secondary electrons in the metal layer are traced separately, until the particular electron either crosses the interface, or arrives at an energy too small to overcome the Schottky barrier.

The interface is simply modeled by an abrupt potential step between the conduction-band minima of metal and semiconductor, and the electrons are treated within the effective-mass approximation, with $m_m/m=1$ for the metal and $m_s/m=0.82$ for GaP [15]. Because of the short mean free path for electron-phonon scattering in the depletion zone [4,12], a 50% chance is assumed that electrons which have already crossed the interface will finally be scattered back into the metal. Therefore, the effective transmission coefficient P_i is assumed to be one-half of the quantum-mechanical result [16]:

$$P_i=\tfrac{1}{2}4k_{\perp m}k_{\perp s}/(k_{\perp m}+k_{\perp s})^2.$$

Here, $k_{\perp m}$ and $k_{\perp s}$ are the perpendicular momenta in the metal and in the semiconductor, respectively. Conservation of the parallel momentum $k_\parallel$ leads to a confinement of $k_\parallel^2\le 2m_s/\hbar^2(E-E_F^m-V_0)$ in the metal, resulting in a finite acceptance cone [6]. V_0 is the effective Schottky-barrier height, which includes a correction for the image potential [15].

After transmission into the semiconductor, the electrons are assumed to contribute to the BEEM current; hence no further tracing of the electron paths is required. In the case of an electron with sufficiently high energy, however, an electron-hole pair may be created by impact ionization that in turn can be separated within the depletion zone, contributing an additional electron to the BEEM current [7]. The probability for such a multiplication effect is approximately given by [10]

$$P_{ii}=1-\exp\left[-S_{ii}\frac{(E-E_F^m-V_0-E_{th})^2}{\sqrt{E-E_F^m-V_0}}\right].$$

To derive this equation, a quadratic energy dependence of the impact-ionization rate is assumed, starting at a threshold energy E_{th}, which is slightly larger than the band gap of the semiconductor [17]. S_{ii} is proportional to the width of the depletion zone and characterizes the strength of impact ionization.

The results of the Monte Carlo simulations are included in Fig. 1, together with subspectra accounting for the different contributions to the BEEM current. Despite the simplicity of the model, an astonishingly good agreement with experiment was obtained. The simulations were per-

formed by successively adjusting the parameters. In this way, angular-distribution widths $\Delta\vartheta_T$ between 15° and 25° were found. Inelastic scattering is described by $\lambda_{in}^0 = 510$ ÅeV^2 for Au and $\lambda_{in}^0 = 85$ ÅeV^2 for Mg, and the mean free path for elastic scattering was found to be $\lambda_{el} = 30$ Å for both Au and Mg. These path lengths have an estimated error of $\pm 30\%$, mainly due to the inaccuracy in the absolute film thicknesses. For the best fits of the thin-film spectra, the local metal thicknesses used in the Monte Carlo simulations were slightly adjusted within the corrugation amplitudes of the topographic images. Impact ionization is characterized by $S_{ii} = 2 \pm 1$ $eV^{-3/2}$ and $E_{th} = 3.0 \pm 0.5$ eV, where the errors reflect the range in which data and simulation show reasonable agreement. The effective Schottky-barrier heights V_0, which were determined by fitting the BEEM spectra in the threshold region with a thermally broadened $\frac{5}{2}$ power law [18], show a slight thickness dependence and are discussed elsewhere [10].

The Monte Carlo simulations reflect both the absolute magnitude and the main spectral features of the BEEM current in an excellent way. The strong variations in spectral shape at $V_T < 4$ eV are mainly due to the energy dependence of the mean free path for inelastic scattering, resulting in a decrease of the contribution of ballistic electrons at high tip voltages; this accounts for the overshoot of the BEEM current for 50 Å Mg. The energies of those electrons which have lost energy by inelastic scattering in the metal usually fall below the threshold for impact ionization. Thus, the strong increase in BEEM current at $V_T \cong 4$ eV due to impact ionization (see dash-dotted subspectra) is only observed when inelastic scattering is weak enough to allow the electrons to reach the interface ballistically. In this way, the BEEM current reaches even 40% of the tunnel current in the case of 12 Å Au. In the case of 50 Å Mg, on the other hand, impact ionization plays no role at all.

The mean free path for elastic scattering, which mainly results from the magnitude of the BEEM current, is found to be rather small, even smaller than that reported by Schowalter and Lee for Au/Si(111) [4]. This may be due to a different chemical composition of the metal layer because of interfacial reactions [14]. Thus a larger λ_{el} might be expected for thicker metal films, an effect that was not found in our simulations. Furthermore, it is observed that the ballistic contributions usually dominate over the elastically scattered contributions, since elastic scattering leads to larger average path lengths through the metal film, as well as to higher incident angles at the interface causing total reflection.

At this point, we like to point out that the width of the acceptance cone at the interface, which is a crucial parameter in the Monte Carlo simulations, might be underestimated within the present model. Kinematically, the band structure of GaP [19] allows complete acceptance already at $\simeq 0.5$ eV above threshold. With a corresponding modification of our model, however, the BEEM spectra could not be simulated with reasonable parameter sets. In particular, extremely low elastic mean free paths or transmission probabilities would have to be assumed, and the BEEM images discussed below could not be simulated. This result suggests that dynamics cannot be neglected, which accounts for finite angular acceptance up to higher energies. In this context, it cannot be excluded that the observed threshold assigned to impact ionization is—at least partially—due to an increase in transmission probability resulting from a peak in the density of states of GaP [7,19]. These observations demonstrate that more elaborate theoretical treatments of interface transmission similar to those performed by Stiles and Hamann for epitaxial interfaces with Si [2,3] are needed.

In Figs. 2(a) and 2(b), a topographic image of (12 Å Au)/GaP(110) is shown, together with a simultaneously recorded BEEM-current image. In order to emphasize correlations, contour lines of metal-film thickness and surface gradient from the topographic image as well as

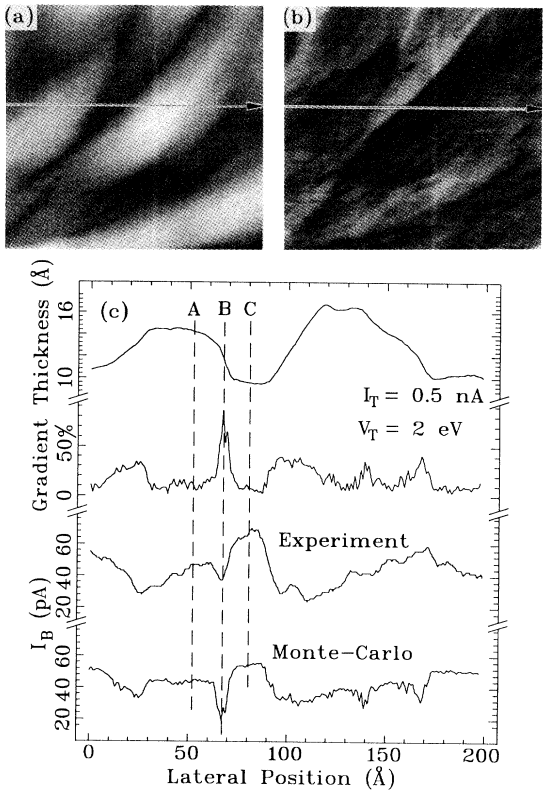

FIG. 2. (a) Topographic image of a 200 Å×200 Å area of 12 Å Au on *n*-type GaP(110), taken with $I_T = 0.5$ nA and $V_T = 2$ eV, with a grey-shade contrast of 10 Å, corresponding directly to local film thicknesses ranging from 7 to 17 Å. (b) Simultaneously recorded image of the BEEM current I_B ranging from 20 to 100 pA. (c) Contour lines, taken along the arrows, of local film thickness and surface gradient (i.e., the tangents of the slope angle between surface and interface), as well as measured and calculated BEEM current.

from the BEEM-current image are given in Fig. 2(c). The influence of topography on the BEEM current is clearly seen: Comparing positions A and C, there is a strong dependence on film thickness. While A is about 5 Å higher than C, the BEEM current is reduced to about 70%. At position B, in the presence of a large surface gradient, the BEEM current decreases strongly to about 60% of the value expected in the absence of a surface gradient. A similar influence of the surface gradient on the BEEM current had been reported previously for Mg/GaP(110) [18].

The dependence of the BEEM current on both local metal-film thickness and surface gradient can also be quantitatively described by the Monte Carlo simulations, using as input parameters the same values as above, and local film thicknesses and surface gradients from the topographic image. In Fig. 2(c), the calculated BEEM current is plotted beneath the corresponding contour line of the experimental data. The remarkable agreement between theory and experiment indicates that the topography of the metal surface accounts for most of the observed inhomogeneities in the BEEM image. The decrease of the BEEM current with increasing surface gradient is well explained by enhanced total reflection at the interface due to the finite acceptance cone. It should be noted that the increase in path length through the metal film alone, without taking the acceptance cone into account, cannot explain the observed effects to the full extent. On the other hand, grain boundaries or other inhomogeneities in the metal film, which may cause lateral variations in scattering, may also account for the observed gradient effect or at least for the minor discrepancies between the two curves. On the basis of the present data, however, an ultimate assignment is not feasible, and more detailed studies using more homogeneous metal films are required.

In conclusion, we have shown that BEEM spectra up to tip voltages of 6 eV as well as BEEM-current images for Au and Mg on n-type GaP(110) can be described by Monte Carlo simulations. The remarkable agreement with experiment demonstrates the capability of the model applied to electron transport from tip to semiconductor. By simulating BEEM spectra for various metal-film thicknesses, the mean free paths for elastic and inelastic scattering as well as parameters describing tunneling and impact ionization within the semiconductor are obtained. Since the present model is partly based on rather simple approximations, however, more sophisticated theories are needed for full understanding of transport processes in BEEM experiments.

The authors thank Professor M. Scheffler and Professor F. Forstmann for valuable discussions on theoretical aspects. This work was supported by the Deutsche Forschungsgemeinschaft, projects Sfb-6/TPA01 and Pr289/2-1. One of us (M.T.C.) gratefully acknowledges support from the Consejo Superior de Investigaciones Cientificas, Spain.

*On leave from the Instituto de Ciencia de Materiales, CSIC, Serrano 144, E-28006 Madrid, Spain.

[1] W. J. Kaiser and L. D. Bell, Phys. Rev. Lett. **60**, 1406 (1988).
[2] M. D. Stiles and D. R. Hamann, Phys. Rev. Lett. **66**, 3179 (1991).
[3] M. D. Stiles and D. R. Hamann, J. Vac. Sci. Technol. B **9**, 2394 (1991).
[4] L. J. Schowalter and E. Y. Lee, Phys. Rev. B **43**, 9308 (1991); E. Y. Lee and L. J. Schowalter, J. Appl. Phys. **70**, 2156 (1991).
[5] E. Y. Lee and L. J. Schowalter, J. Appl. Phys. **70**, 2156 (1991).
[6] R. Ludeke, M. Prietsch, and A. Samsavar, J. Vac. Sci. Technol. B **9**, 2342 (1991).
[7] R. Ludeke, Phys. Rev. Lett. **70**, 214 (1993).
[8] M. Prietsch, A. Samsavar, and R. Ludeke, Phys. Rev. B **43**, 11850 (1991).
[9] M. Prietsch, Habilitationsschrift, Freie Universität Berlin, 1992 (unpublished).
[10] A. Bauer, M. T. Chuberes, M. Prietsch, and G. Kaindl, J. Vac. Sci. Technol. B (to be published).
[11] J. G. Simmons, J. Appl. Phys. **35**, 2655 (1964).
[12] C. R. Crowell and S. M. Sze, in *Physics of Thin Films*, edited by G. Hass and R. F. Thun (Academic, New York, 1967), Vol. 4, p. 325.
[13] J. B. Pendry, in *Photoemission and the Electronic Properties of Surfaces*, edited by B. Feuerbacher, B. Fitton, and R. F. Willis (Wiley, New York, 1978).
[14] R. Ludeke, A. B. McLean, and A. Taleb-Ibrahimi, Phys. Rev. B **42**, 2982 (1990); M. T. Cuberes, A. Bauer, M. Prietsch, and G. Kaindl (unpublished).
[15] S. M. Sze, *Physics of Semiconductor Devices* (Wiley, New York, 1984), 2nd ed.
[16] E. Merzbacher, *Quantum Mechanics* (Wiley, New York, 1962), p. 86.
[17] E. A. Eklund, P. D. Kirchner, D. K. Shuh, F. R. McFeely, and E. Cartier, Phys. Rev. Lett. **68**, 831 (1992).
[18] M. Prietsch and R. Ludeke, Phys. Rev. Lett. **66**, 2511 (1991).
[19] J. R. Chelikowsky and M. L. Cohen, Phys. Rev. B **14**, 556 (1976).

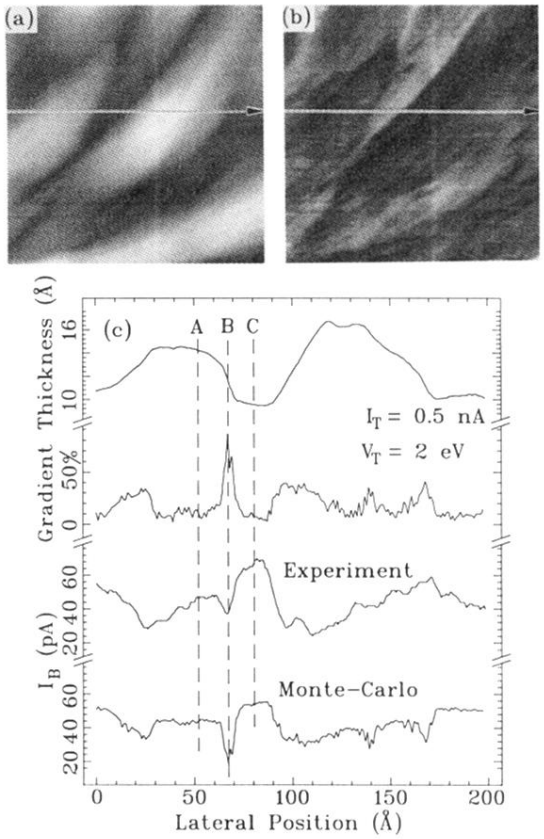

FIG. 2. (a) Topographic image of a 200 Å×200 Å area of 12 Å Au on *n*-type GaP(110), taken with I_T=0.5 nA and V_T=2 eV, with a grey-shade contrast of 10 Å, corresponding directly to local film thicknesses ranging from 7 to 17 Å. (b) Simultaneously recorded image of the BEEM current I_B ranging from 20 to 100 pA. (c) Contour lines, taken along the arrows, of local film thickness and surface gradient (i.e., the tangents of the slope angle between surface and interface), as well as measured and calculated BEEM current.